ANTIOXIDANTS & REDOX SIGNALING
Volume 14, Number 7, 2011

DOI: 10.1089/ars.2010.3421

Enhanced ROS Generation Mediated by Alzheimer's Disease Presenilin Regulation of $InsP_3R$ Ca^{2+} Signaling

Marioly Müller,[1,*] King-Ho Cheung,[1,*] and J. Kevin Foskett[1,2]

Abstract

Familial Alzheimer's disease (FAD) is caused by mutations in amyloid precursor protein and presenilins (PS1, PS2). Many FAD-linked PS mutations affect intracellular calcium (Ca^{2+}) homeostasis by proximal mechanisms independent of amyloid production by dramatically enhancing gating of the inositol trisphosphate receptor ($InsP_3R$) intracellular Ca^{2+} release channel by a gain-of-function effect that mirrors genetics of FAD and is independent of secretase activity. Electrophysiological recordings of $InsP_3R$ in FAD patient B cells, cortical neurons of asymptomatic PS1-AD mice, and other cells revealed they have higher occupancy in a high open probability burst mode, resulting in enhanced Ca^{2+} signaling. Exaggerated Ca^{2+} signaling through this mechanism results in enhanced generation of reactive oxygen species, believed to be an important component in AD pathogenesis. Exaggerated Ca^{2+} signaling through $InsP_3R$–PS interaction is a disease specific and robust proximal mechanism in AD that may contribute to the pathology of AD by enhanced generation of reactive oxygen species. *Antioxid. Redox Signal.* 14, 1225–1235.

Introduction

Alzheimer's disease (AD) is a common form of dementia involving slowly developing and ultimately fatal neurodegeneration. Age is the main risk factor but the major molecular mechanisms are still unclear. A hallmark feature of AD is accumulation of extracellular β amyloid (Aβ) plaques, intracellular neurofibrillary tangles, and neuronal loss (19). Mutations in presenilins (PS1 and PS2) and amyloid precursor protein (APP) cause most early-onset, autosomal dominant familial cases of the disease (FAD) (73). Presenilins are transmembrane proteins that are synthesized and localized in the endoplasmic reticulum (ER) membrane (1). Together with nicastrin, APH-1, and PEN-2, PS forms a protein complex that is transported to the cell surface and endosomes, where it functions as a γ-secretase that cleaves several type 1 transmembrane proteins, including APP (14, 45). Mutant PS are believed to affect APP processing by either enhancing the total production of Aβ or the relative proportion of the more amyloidogenic Aβ-42 form (77). In the amyloid hypothesis of AD, accumulation of amyloidogenic Aβ aggregates or oligomers due to defective processing and clearance is a proximal feature that causes neural toxicity leading to brain pathology (27, 29). Identification of three components in FAD: PS1, PS2, and APP that are linked in a biochemical pathway that impinges on Aβ production has strongly influenced acceptance of the amyloid hypothesis (29).

Disrupted intracellular Ca^{2+} homeostasis has also been implicated in AD. Extracellular Aβ influences intracellular Ca^{2+} homeostasis *in vitro* (33, 53) and *in vivo* (6, 7, 38, 39). In addition to disrupting APP processing, many FAD-linked PS mutations have been shown to affect Ca^{2+} homeostasis by Aβ independent mechanisms (40, 64). Ca^{2+} signaling disruptions associated with expression of FAD PS have been manifested as attenuated capacitive Ca^{2+} entry (30, 41, 78), but most usually as exaggerated Ca^{2+} release from the ER (30, 43, 65, 70, 72), the major intracellular Ca^{2+} storage organelle. The mechanisms underlying exaggerated ER Ca^{2+} release have been ascribed to enhanced loading of the ER lumen (65) due to disruption of a putative Ca^{2+} channel function of wild-type PS (54, 75) or to enhanced activity of the SERCA Ca^{2+} pump (23). Exaggerated Ca^{2+} release has also been accounted for by enhanced Ca^{2+} liberation from normal stores through ryanodine receptor (RyR) (10, 64, 71) and inositol trisphosphate receptor ($InsP_3R$) (43, 68) Ca^{2+} release channels. The latter phenotypes have been observed both *in vivo* (10, 65, 70, 71) and *in vitro* (17, 31, 35, 42). Enhanced release from normal stores has been attributed either to enhanced Ca^{2+} release channel expression (10, 11, 36, 72) or, in the case of the $InsP_3R$, to enhanced activity in response to its ligand $InsP_3$ (12, 13, 35). Regarding the latter, it is notable that enhanced agonist-induced $InsP_3R$-mediated Ca^{2+} signals have been used diagnostically to identify FAD patient cells (31, 35). A biochemical interaction of the $InsP_3R$ with both wild-type (WT) as well as

Department of [1]Physiology and [2]Cell and Developmental Biology, University of Pennsylvania, Philadelphia, Pennsylvania.
*These authors contributed equally to this work.

FAD mutant PS1 and PS2 has been demonstrated (13). Furthermore, single channel recordings of $InsP_3R$ have shown that FAD mutant PS1 and PS2 expression is associated with an apparent sensitization of the $InsP_3R$ channel to $InsP_3$, resulting in enhanced $InsP_3R$ Ca^{2+} release channel gating (13). The single channel studies were performed in the absence of Aβ or cellular pathology, suggesting that modulation of $InsP_3R$ channel gating is a fundamental mechanism that contributes to exaggerated Ca^{2+} signaling in FAD PS-expressing cells.

Here, we review recent data that suggest that enhanced $InsP_3R$ channel gating and resulting exaggerated Ca^{2+} signaling caused by biochemical and functional interactions of FAD PS and $InsP_3R$ is a disease specific and robust proximal mechanism in AD. In addition, new data are presented that show that exaggerated Ca^{2+} signaling through this mechanism results in enhanced generation of reactive oxygen species (ROS), believed to be an important component in AD pathogenesis (21, 49, 59, 66).

Materials and Methods

Cell culture

DT40 cells stably expressing PS1-WT or PS1-M146L were created and maintained as described (13). B-lymphoblast lines derived from human FAD patients and normal individuals (Coriell Institute, Camden, NJ) were maintained at 37°C (95/5% air/CO_2) in RPMI 1640 (Invitrogen, Carlsbad, CA) supplemented with 15% fetal bovine serum (Hyclone, Logan, UT), 2 m*M* L-glutamine, 100 units/ml penicillin, and 100 μg/ml streptomycin.

Calcium imaging

Human B-lymphocytes (Coriell Institute) were plated onto a CellTek-(BD Biosciences, San Jose, CA) coated glass-bottom perfusion chamber mounted on the stage of an inverted microscope (Eclipse TE2000; Nikon, Melville, NY) and incubated with fura-2 AM (2 μ*M*; Invitrogen) for 30 min at room temperature in Hanks' balanced salt solution (HBSS, Sigma, St. Louis, MO) containing 1% BSA. Cells were then continuously perfused with HBSS containing 1.8 m*M* $CaCl_2$ and 0.8 m*M* $MgCl_2$ (pH 7.4). Ca^{2+} signals were elicited by cross-linking the B cell receptor (BCR) with 50 ng/ml anti-human IgM antibody (Southern Biotech, Birmingham, AL). In some experiments, cells were perfused with complete culture medium containing 10% FBS. Fura-2 was alternately excited at 340 and 380 nm, and the emitted fluorescence filtered at 510 nm was collected and recorded (13, 76) using a CCD-based imaging system running Ultraview software (Perkin Elmer, Waltham, MA). Dye calibration was achieved by applying experimentally determined constants to the standard equation $[Ca^{2+}] = K_d \cdot \beta \cdot (R - R_{min})/(R_{max} - R)$.

Electrophysiology

Preparation of isolated nuclei from cells was performed as described (13, 46, 76). In brief, cells were washed twice with PBS and suspended in nuclear isolation solution containing (in m*M*): 150 KCl, 250 sucrose, 1.5 β-mercapoethanol, 10 Tris-HCl, 0.05 phenylmethylsulphonyl fluoride, and protease inhibitor cocktail (Complete, Roche Diagnosis, Indianapolis, IN), pH 7.3. Nuclei were isolated using a Dounce glass homogenizer and plated onto a 1-ml glass-bottomed dish containing standard bath solution (in m*M*): 140 KCl, 10 HEPES, 0.5 BAPTA, and 0.192 $CaCl_2$ (free $[Ca^{2+}] = 90$ n*M*). The pipette solution contained (in m*M*): 140 KCl, 10 HEPES, 0.5 dibromo-BAPTA, and 0.001 free Ca^{2+}, pH 7.3. Free $[Ca^{2+}]$ in solutions was adjusted by Ca^{2+} chelators with appropriate affinities and confirmed by fluorometry as described (13). Data were recorded at room temperature and acquired using an Axopatch 200A amplifier (Molecular Devices, Sunnyvale, CA), filtered at 1 kHz, and digitized at 5 kHz with an ITC-16 interface (Instrutech) and Pulse software (HEKA Instruments Inc., Bellmore, NY).

Hydrogen peroxide generation measurements

DT40 cells stably expressing PS1-WT or PS1-M146L were washed twice with HBSS and suspended in 2 ml HBSS. Amplex Red reagent and HRP were added and the fluorescence intensity was monitored continuously for 20 min (PTI QuantaMaster fluorimeter; Photon Technology Intl, Birmingham, NJ; ex: 530 nm, em: 590 nm). The increase in fluorescence intensity over 20 min in control DT40 cells was used to normalize signals from PS-expressing cells. PC12 cells were transiently transfected with pIRES-EGFP, pIRES-GFP-PS1WT, or pIRES-GFP-M146L and grown in 6-well plates for 48 h. Cells were washed twice in HBSS and suspended in 2 ml HBSS. Amplex Red reagent and HRP were added to the incubation medium and the fluorescence intensity of the supernatant was measured after 30 min. Fluorescence intensity was calculated as $(F - F_o)/([protein])/F_{GFP}$, where F is the fluorescence intensity of the cell supernatant, F_o is the fluorescence intensity of the supernatant without cells, and F_{GFP} is the fluorescence intensity of the cell supernatant in pIRES-EGFP empty vector transfected cells. In some experiments, PC12 cells were treated with 10 μ*M* BAPTA-AM for 30 min to chelate the intracellular Ca^{2+} stores prior to addition of Amplex Red reagents.

Analysis and Statistics

Data were summarized as the mean $\pm$ S.E.M. and the statistical significance of differences between means was assessed using unpaired *t*-tests or analysis of variance (ANOVA) for repeated measures. Differences between means were accepted as statistically significant at the 95% level ($p < 0.05$).

Results

FAD PS enhancement of $InsP_3R$ gating is a robust phenotype observed in many cells

By co-immunoprecipitation from transfected cells and mouse brain lysates, biochemical interactions of WT and FAD mutant PS1 and 2 with the $InsP_3R$ were identified (12, 13). Functionally, FAD PS had gain-of-function consequences for the activity of the channel that were not observed for WT PS, and which in turn were associated with exaggerated $[Ca^{2+}]_i$ signaling in intact cells (12, 13). FAD and WT PS1 were stably expressed in chicken DT40 cell pre-B lymphocytes, and patch clamp experiments were performed on isolated nuclei to record $InsP_3R$ ion channels in their native membrane (46). No novel ion channel activities were observed in nuclei from the wild-type (WT) or mutant PS1-expressing native DT40 cells (13). In saturating $[InsP_3]$, PS1-WT was without effect on single $InsP_3R$ channel activity channel (channel open probability

$P_o = 0.53$ in control versus 0.57 in PS1-WT expressing cells), whereas PS1-M146L expression increased channel activity ($P_o = 0.83$; $p < 0.01$; Figs. 1A and 1C) by locking the channel open for long periods (Fig. 1D). In suboptimal [$InsP_3$] (100 n*M*), mutant PS1 stimulated the channel activity by four fold ($P_o = 0.63$ versus 0.16 for control cells; Figs. 1B and 1C) to levels similar to those observed for control channels in saturating [$InsP_3$] (13). Similar results were obtained with an FAD PS2 mutant (N141I) (12, 13).

Enhanced $InsP_3R$ channel activity appears to be a conserved feature of FAD PS-expressing cells, since similar results were observed in cells expressing other FAD mutant PS (12). γ-secretase-dead mutants also significantly enhanced $InsP_3R$ channel activity, although to a lesser extent than the FAD mutants, indicating that the secretase activity of PS is not required for its effects on $InsP_3R$ gating (12). Importantly, P_o of channels recorded from cells infected with frontotemporal dementia-associated mutant PS1 was not different from controls (12). Thus, several FAD-mutant PS have similar effects on $InsP_3R$ gating, and these effects appear not to be recapitulated in PS mutants associated with a different neurological disease.

These effects of FAD PS on $InsP_3R$ gating appear to be remarkably robust, since they have now been observed in five different cellular systems: Sf9 cells, chicken DT40 B cells, human FAD patient B lymphoblasts and fibroblasts, and neurons from FAD-PS AD mice, in the absence of and preceding disease pathology (12, 13). The strikingly similar effects of mutant PS expression of $InsP_3R$ channels in such diverse cellular systems from different species suggest that they are robust in all cell types and for all $InsP_3R$ isoforms. The electrophysiological studies suggest that FAD PS stimulate $InsP_3R$ gating by a mechanism that involves PS-mediated effective sensitization of the channel to $InsP_3$, most likely through an allosteric mechanism. Modal gating analysis suggested that FAD mutant PS regulate channel activity by impinging upon the normal ligand activation mechanisms (12). Ligand regulation of $InsP_3R$ gating is largely mediated by altering propensity of the channel to gate in particular modes (34). Strongly activated channels gate in a high-P_o H mode characterized by long bursting activities; an intermediate-P_o I mode is characterized by fast channel openings and closings; and a low-P_o L mode characterized by long closings with brief openings. FAD PS appear to impinge on modal gating. $InsP_3R$ gating was examined in lymphoblasts from three human FAD patients harboring PS1-M146L, PS1-A246E, or PS2-N141I, as well as from two different age-matched unaffected individuals. $InsP_3R$ from the two unaffected individuals had similar low channel P_o (0.18 and 0.23, respectively; Figs. 2A and 2B) with channel activities characterized by brief openings with relatively long closings (Figs. 2A and 2C). Strikingly, $InsP_3R$ P_o recorded from all three FAD patients were profoundly elevated by 2–3-fold when compared with the unaffected individuals (PS1-M146L: 0.62; PS1-A246E: 0.67; PS2-N141I: 0.50; Figs. 2A and 2B), mainly due to a marked decrease in the mean channel closed time t_c (Fig. 2C), with many channels observed to be bursting for extended periods (Fig. 2E). In cells from unaffected individuals, the L and I gating modes dominated channel kinetics, whereas $InsP_3R$ recorded from FAD patient lymphoblasts spent 50%–75% of the time in the high P_o H mode (Figs. 2D and 2E). Analogous results were obtained with low (100 n*M*) $InsP_3$. $InsP_3R$ P_o was 0.04 in an unaffected individual, whereas P_o was increased by five-fold to 0.22 in cells from the PS1-A246E patient (Figs. 2F and 2G).

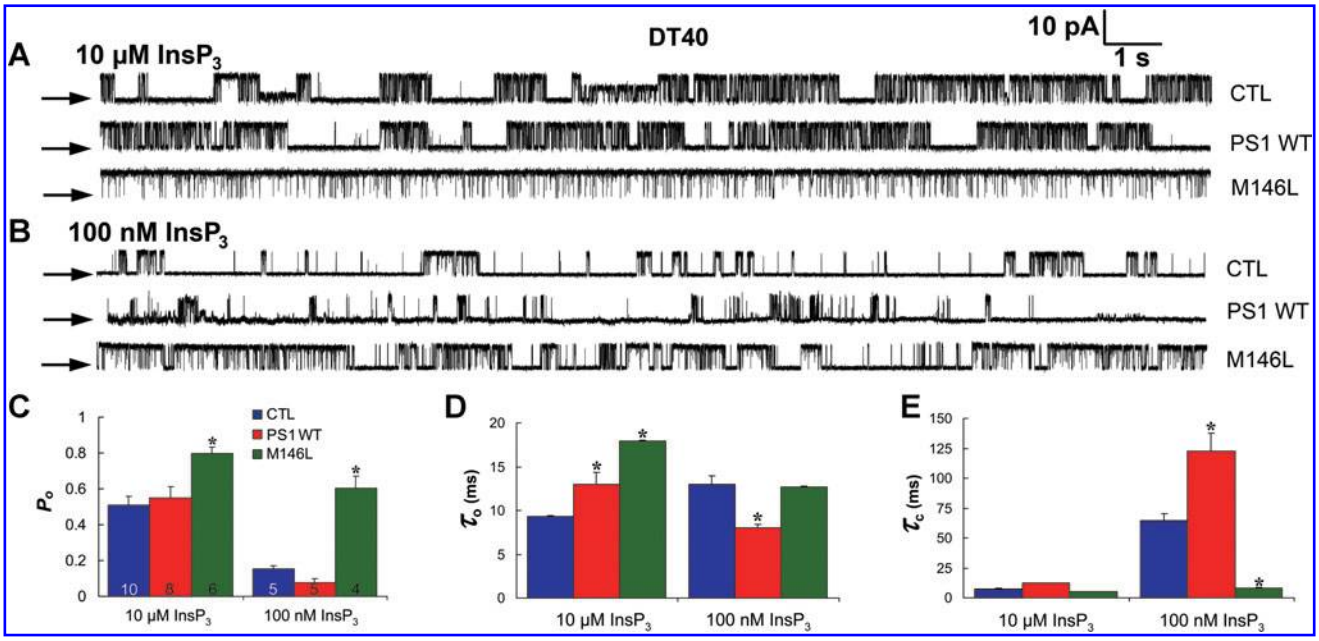

FIG. 1. Effects of PS1 expression on $InsP_3R$ single channel activity in DT40 cells. Representative $InsP_3R$ single-channel current recordings in presence of saturating (10 μM; **A)** or sub-saturating (100 n*M*; **B)** $InsP_3$ in DT40 cells stably transfected with PS1 WT or M146L. Pipette [Ca^{2+}] was 1 μM, optimal for channel activity; *arrows*: zero current level. Summary of effects of PS1 expression on $InsP_3R$ P_o **(C)**, mean open time (t_o) **(D)**, and mean closed time (t_c) **(E)**. *Asterisks*: $p < 0.01$, unpaired *t*-test. From Cheung *et al*. (13) with permission from Elsevier. (For interpretation of the references to color in this figure legend, the reader is referred to the web version of this article at www.liebertonline.com/ars).

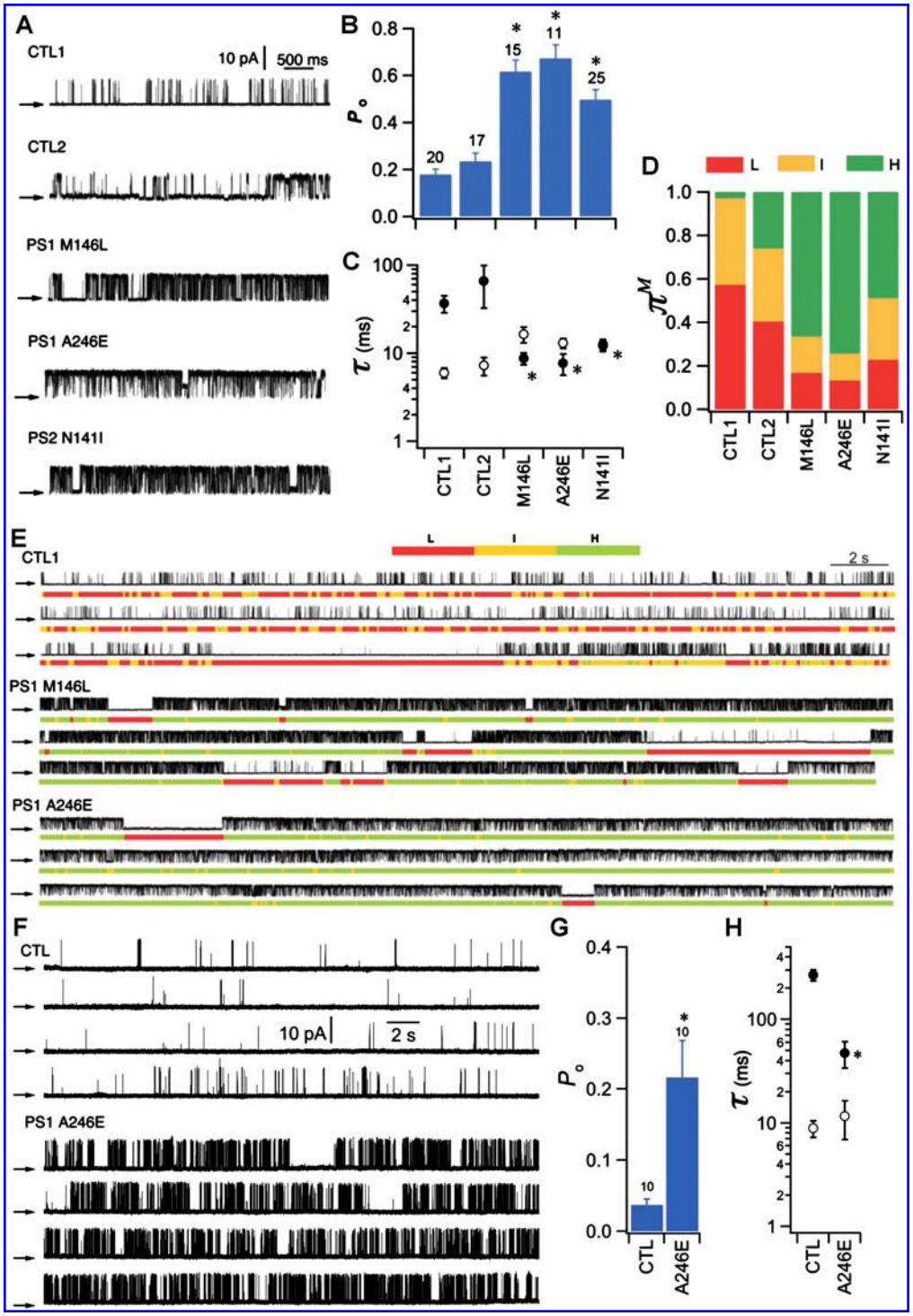

FIG. 2. Effects of FAD PS on $InsP_3R$ gating in human FAD patient B lymphoblasts. (A) Representative human $InsP_3R$ current traces at +20 mV in isolated nuclei from human FAD lymphoblasts and control lymphobalsts from age-matched individuals without FAD activated with 10 μM $InsP_3$ and 1 μM Ca^{2+} in pipette solution. Summary of $InsP_3R$ channel P_o **(B)**, τ_o (*open circle*) and τ_c (*filled circle*) **(C)** and modal gating analysis **(D)** from different human lymphoblasts. *Asterisks*: $p < 0.05$ by ANOVA compared with CTL1. **(E)** Modal gating analyses of $InsP_3R$ channel from human lymphoblasts. Distinct human $InsP_3R$ gating behaviors in unaffected normal individual *vs* FAD lymphoblasts with PS1 mutations. Each section shows continuous recording with gating mode assignment in color code below it. In cells from normal individuals, low channel P_o is associated with switching between L and I modes. In cells from all three individuals with FAD, enhanced $InsP_3R$ gating is manifested by increased occupancy of the H mode at the expense of L mode. **(F–H)** Single $InsP_3R$ channel current traces from human lymphoblasts activated by suboptimal $InsP_3$. **(F)** Representative current traces (+20 mV) in isolated nuclei from human FAD lymphoblasts and age-matched control B lymphoblasts activated by suboptimal 100 nM $InsP_3$ and 1 μM Ca^{2+}. Summary of $InsP_3R$ channel P_o **(G)**, and τ_o (*open circle*) and τ_c (*filled circle*) **(H)** from aged-matched control and FAD human B-lymphocytes. *Asterisks*: $p < 0.05$ by Student's *t*-test. From Cheung *et al*. (12) with permission from the American Association for the Advancement of Science. (For interpretation of the references to color in this figure legend, the reader is referred to the web version of this article at www.liebertonline.com/ars).

These observations in human B-lymphoblasts with endogenous levels of PS and $InsP_3R$ are remarkably similar to those observed in single $InsP_3R$ channel recordings in nuclei isolated from insect Sf9 cells, DT40 cells, and embryonic cortical neurons from transgenic mice with human FAD PS1 knocked into the mouse PS1 locus (12, 13). FAD PS enhance $InsP_3R$ gating by mode switching, causing the channel to spend more time in the H mode. Modal gating regulation may have important functional consequences. The channel open time in the L mode is ~10 ms, which may not be long enough for Ca^{2+} flux through the channel to increase local $[Ca^{2+}]$ sufficiently to recruit additional $InsP_3R$- or RyR-mediated Ca^{2+} release by Ca^{2+}-induced Ca^{2+} release (CICR). In contrast, the much longer openings in the H mode (>200 ms) can provide a large Ca^{2+} flux to enable a normally local Ca^{2+} signal to be amplified and propagated by CICR (20). It was suggested (12) that because $InsP_3R$ and RyR are clustered and spatially organized to provide local $[Ca^{2+}]_i$ signals as a critical element of physiological specificity, mode-shifting by FAD PS may result not only in exaggerated local Ca^{2+} signaling, but also disruption of spatial specificity by enabling CICR to transmit signals more globally (20, 34). Mode switching by FAD PS of $InsP_3R$ gating may account for observations $InsP_3$ dependent exaggerated RyR mediated Ca^{2+} signals in neurons (*e.g.*, (71, 72)).

The effects of FAD PS on $InsP_3R$ gating result in altered $[Ca^{2+}]_i$ signaling

The effects of FAD PS expression on the behavior of the $InsP_3R$ measured at the single channel level are consistent with the observations of exaggerated $InsP_3$-mediated $[Ca^{2+}]_i$ signals in FAD patient fibroblasts (35) and other cells with mutant PS expressed (68, 69). To address whether the effects observed at the single-channel level were associated with altered $[Ca^{2+}]_i$ signaling, $InsP_3R$-mediated Ca^{2+} signals were measured in the same human FAD patient B cell-derived lymphoblasts that were used for single-channel studies. $InsP_3R$-mediated Ca^{2+} signals were elicited by cross-linking the B cell receptor (BCR) with IgM antibody. With strong stimulation (5 μg/ml), 20% of cells from both control individual and an FAD patient responded with similar $[Ca^{2+}]_i$ oscillations and spiking (Figs. 3B and 3D), whereas a further 27% of FAD patient cells responded with exaggerated high-level transient responses (Figs. 3A–3C). With weak stimulation (50 ng/ml), $[Ca^{2+}]_i$ oscillations and spiking were triggered in ~20% of control cells (Figs. 3E and 3G), due to periodic Ca^{2+} release through the $InsP_3R$, whereas in cells isolated from FAD patients, both the number of responding cells as well as the oscillation/spiking frequency were increased (Figs. 3E, 3G, and 3H). Perfusion with normal culture medium containing serum that generates low-level $InsP_3$ production (76) induced spontaneous $[Ca^{2+}]_i$ oscillations/spiking in ~25% of control patient cells (Figs. 3F and 3G). In contrast, the number of PS1 FAD patient B lymphoblasts displaying spontaneous Ca^{2+} oscillations was increased by 100% and the oscillation/spiking frequency doubled (Figs. 3F–3H). These responses are consistent with an enhanced sensitivity and activity of $InsP_3$-mediated Ca^{2+} release in human FAD patient cells, in concordance with enhanced $InsP_3R$ channel activity recorded in the same cells.

FAD PS-mediated enhanced $[Ca^{2+}]_i$ signaling causes enhanced ROS production

$InsP_3$-mediated $[Ca^{2+}]_i$ signals regulate many cell physiological processes. A major question is whether the effects of FAD mutant PS on $InsP_3R$-mediated Ca^{2+} signaling have relevance for disease pathogenesis. It is possible that exaggerated Ca^{2+} signals in AD may influence mitochondrial function, gene transcription, and Aβ production (57), features associated with AD. Ca^{2+} released from the ER through the $InsP_3R$ can be rapidly taken up by mitochondria located in close proximity (60). Periodic release of Ca^{2+} from the ER stimulates mitochondrial enzymes of the TCA cycle, leading to the maintenance of efficient oxidative phosphorylation and ATP production (15, 28). However, in response to excess Ca^{2+} release, the Ca^{2+}-induced increase in mitochondrial NADH can exceed that needed to sustain oxidative phosphorylation, and lead to an electron-saturated respiratory chain that results in increased mitochondrial ROS production. Oxidative stress has been invoked in AD and as a link between aging and neurodegeneration (22, 48, 55, 56). The identification of the $InsP_3R$ as a molecular target of PS regulation suggests a mechanism that may link mutations in PS to enhanced oxidative stress.

Because elevated rates of mitochondrial electron transport result in enhanced generation of superoxide that is rapidly dismutated to H_2O_2 that leaks through plasma membranes to the extracellular solution, we measured ROS production by recording the amount of H_2O_2 released from cells under basal conditions and in response to agonist stimulation. Stable expression of either PS1-WT or PS1-M146L did not affect the basal production of H_2O_2 by DT40 cells (Figs. 4A and 4B). In contrast, BCR stimulation with a low dose of IgM (0.05 μg/ml) significantly enhanced H_2O_2 production in PS-expressing cells, most markedly in the PS1-M146L-expressing cells (Figs. 4A and 4B). Enhanced H_2O_2 production observed in PS1-expressing cells was entirely dependent on the expression of $InsP_3R$, because it was absent in $InsP_3R$-deficient DT40-KO cells (Fig. 4C). These results indicate that the agonist-stimulated production of ROS and, importantly, the potentiation by mutant PS1, are caused by $InsP_3R$-mediated Ca^{2+} release.

Analogous experiments were performed in neuronal PC12 cells transfected (efficiency ~50%) with either *PS1-WT* or *PS1-M146L* cDNAs, and stimulated with a high (100 μM) and low (1 μM) dose of ATP to activate P2Y2 receptors (74). The responses observed in PC12 cells with a high dose of ATP were similar to those in DT40 cells, except that basal production of H_2O_2 was enhanced by PS1 expression (Figs. 4D and 4F), with the effect more pronounced in the cells expressing PS1-M146L (Fig. 4F). Because FAD PS effects on $InsP_3R$ channel gating are more pronounced at low levels of $InsP_3$, we also performed experiments using a sub-saturating dose of ATP (1 μM). PC12 cells expressing PS1-M146L generated significantly higher H_2O_2 than either control or PS1-WT cells (Fig. 4F). The agonist-induced elevations of H_2O_2 production were completely inhibited in cells loaded with BAPTA to buffer changes in $[Ca^{2+}]_i$ (Fig. 4E). These results indicate that FAD-associated PS1-M146L promotes ROS production, and the production is dependent on $InsP_3R$-mediated Ca^{2+} release.

Discussion

Whereas observations of disrupted Ca^{2+} signaling in AD have been well documented, the physiological implications of

altered Ca^{2+} signaling and the roles that these changes play in AD pathogenesis are unknown. The identification of the $InsP_3R$ as a molecular mechanism of Ca^{2+} disruption associated with expression of FAD PS may provide new insights. In both DT40 and PC12 cells, expression of PS1-M146L caused an exaggerated ROS production in response to agonists that mobilized Ca^{2+} through the $InsP_3R$. This effect of mutant PS1 was mediated by Ca^{2+} release through the $InsP_3R$ because it was abolished both in cells that lacked $InsP_3R$ expression and by blocking $InsP_3R$-mediated elevations of $[Ca^{2+}]_i$. These results therefore demonstrate that exaggerated Ca^{2+} signals caused by mutant PS1 stimulation of $InsP_3R$ gating result in enhanced ROS generation. Accordingly, the sensitization by mutant PS of the $InsP_3R$ to low $[InsP_3]$ that may exist in unstimulated cells might cause chronically enhanced ROS generation. In agreement, enhanced ROS generation was observed in unstimulated PS1-expressing neuronal PC12 cells. These results therefore suggest a molecular mechanism

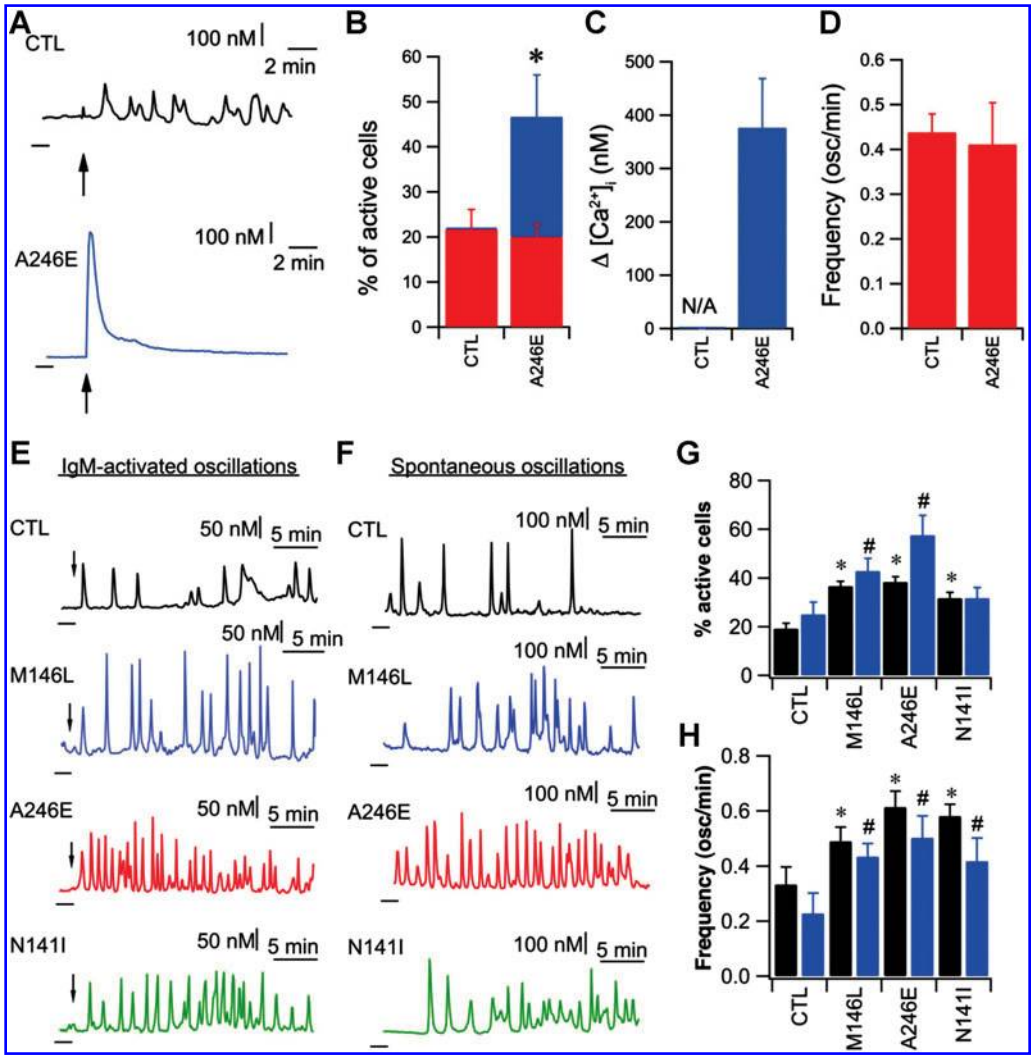

FIG. 3. Exaggerated Ca^{2+} signaling in human FAD B cells. **(A)** Representative single cell Ca^{2+} responses to strong anti-human IgM antibody stimulation (5 μg/ml, added at *arrow*) in control human B-lymphoblasts (CTL) or FAD lymphoblasts carrying PS1-A246E mutation. *Dark lines* below and to the left of each trace indicate zero Ca^{2+}. **(B)** Percentage of cells responding to anti-IgM stimulation. *Red*: percentage responding with Ca^{2+} oscillations; *blue*: percentage responding with large amplitude Ca^{2+} transients. **(C)** Summary of peak amplitudes of high-amplitude transient Ca^{2+} responses triggered by 5 μg/ml anti-IgM. **(D)** Ca^{2+} oscillation frequency in response to anti-IgM. Data summarized from 3 experiments with 30 cells in each experiment. *Asterisk*: $p < 0.05$ by Student's t test. **(E)** Representative single cell Ca^{2+} responses to weak anti-human IgM antibody stimulation (50 ng/ml, added at *arrow*) and **(F)** spontaneous oscillations during perfusion with serum-containing medium in B lymphoblasts from unaffected individuals (CTL) and FAD lymphoblasts with PS1-M146L, PS1-A246E, or PS2-N141I. *Dark lines* indicate zero Ca^{2+} level. **(G)** Summary of percentage of cells responding to anti-IgM stimulation (*black bars*) or undergoing spontaneous Ca^{2+} oscillations in complete medium with serum (*blue bars*). **(H)** Summary of Ca^{2+} oscillation frequency in response to anti-IgM (*black bars*) or spontaneous Ca^{2+} oscillations observed in presence of complete medium (*blue bars*). Data in each group summarized from four experiments with 30 cells in each experiment. *Asterisks* or #: $p < 0.05$ by ANOVA as compared with respective controls. From Cheung *et al.* (12) with permission from the American Association for the Advancement of Science. (For interpretation of the references to color in this figure legend, the reader is referred to the web version of this article at www.liebertonline.com/ars).

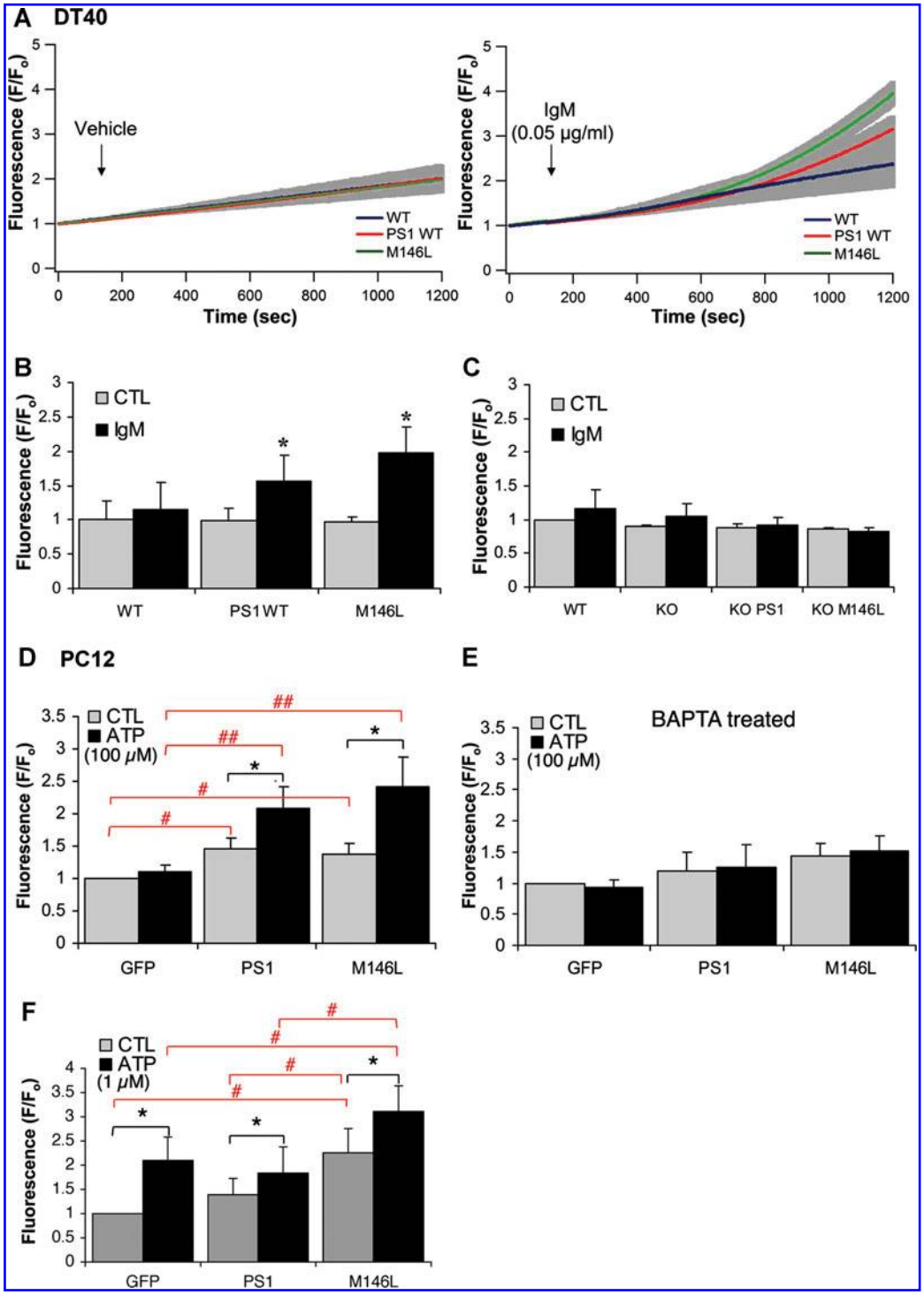

FIG. 4. Effects of PS1 expression on ROS generation in DT40 and PC12 cells. (A) Continuous monitoring of H_2O_2 generation by Amplex Red fluorescence intensity in control (*blue*), and stably transfected PS1-WT (*red*) and M146L (*green*) expressing DT40 lines. *Colored lines* indicate mean intensity of three experiments, and *gray area* shows s.e.m of traces. *Arrows* indicate addition of anti-IgM or vehicle. **(B)** Summary of H_2O_2 generated after 20 min in presence or absence of 50 ng/ml BCR antibody. Amplex Red fluorescence normalized to that observed at time 0 in unstimulated WT cells. **(C)** Summary of H_2O_2 generated after 20 min in presence or absence of 50 ng/ml BCR antibody in $InsP_3R$ KO DT40 lines. Amplex Red fluorescence normalized to that observed at time 0 in unstimulated WT cells. **(D)** Summary of H_2O_2 generated over 30 min in the presence or absence of 100 μM ATP by PC12 cells expressing GFP, PS1-WT, or PS1-M146L. Amplex Red fluorescence normalized to that observed at time 0 in unstimulated GFP-transfected cells. **(E)** Summary of H_2O_2 generated over 30 min in presence or absence of 100 μM ATP by PC12 cells expressing GFP, PS1-WT, or PS1-M146L with or without pretreatment with 10 μM BAPTA-AM. Amplex Red fluorescence normalized to that observed at time 0 in unstimulated GFP-transfected cells. **(F)** Summary of H_2O_2 generated over 30 min in the presence or absence of 1 μM ATP by PC12 cells expressing GFP, PS1-WT, or PS1-M146L. Amplex Red fluorescence normalized to that observed at time 0 in unstimulated GFP-transfected cells. *Single and double asterisks and number symbols* indicate $p < 0.05$ or $p < 0.01$, respectively. (For interpretation of the references to color in this figure legend, the reader is referred to the web version of this article at www.liebertonline.com/ars).

by which mutant PS could exacerbate oxidative stress, independent of effects of Aβ.

ROS are generated at low levels in most cells during oxidative phosphorylation in mitochondria. ROS can also be generated by NADPH oxidase and xanthine oxidase (74), but mitochondria are generally considered to be the source of most ROS in the cell, especially in the brain. Ca^{2+} released from the ER in response to agonist stimulation (61, 67), as well as by constitutive low-level $InsP_3R$ activity (8) can be taken up by mitochondria where it enhances oxidative phosphorylation by stimulation of dehydrogenases to produce NADH, or the F1-F0-ATPase directly (3, 50). What is not clear from our studies are the functional consequences of the enhanced ROS generated as a consequent of FAD PS-mediated enhanced $InsP_3R$ Ca^{2+} release activity that we have observed. ROS at low levels can have important signaling functions (5, 18). For example, ROS generation is important for hippocampal long-term potentiation (LTP) (63), and H_2O_2 can modify the redox state of RyR by increasing its *S*-glutathionylation, potentiating Ca^{2+} release and enhancing ERK and CREB phosphorylation that may impinge on gene transcription (37). Alternately, excessive ROS generation can damage proteins, lipids, and DNA. Excessive ROS generation and neurodegeneration have been linked in many studies (4, 62). Oxidative stress can trigger cell cycle activation in mature neurons, and such activation leads to cell death (32). A large body of evidence indicates that damage from ROS is a common and prominent feature in the brain in AD (21, 49, 59, 66). Aging is the major risk factor for nonfamilial forms of AD, and cumulative cellular damage caused by mitochondrial ROS generation is the basis of the "mitochondrial theory" of aging (52). Brain metabolism is reduced in AD and the activities of several mitochondrial enzymes are diminished (49, 59, 66). It has been proposed that these features may be a consequence of mitochondrial damage due to oxidative stress (22). Accordingly, excessive ROS production associated with FAD PS expression may accelerate this process. Several studies have suggested that therapeutic antioxidant strategies may be beneficial in AD (22, 55). Much of the focus on ROS in AD has been on Aβ, and its association with increased production of ROS and impairment of anti-oxidant defenses (2, 47, 58). ROS responses of cells to exogenous Aβ are enhanced in cells expressing FAD mutant PS (24–26). Nevertheless, some evidence suggests that oxidative stress in the brain may be an early event that precedes even mild cognitive decline (55). Furthermore, enhanced ROS generation has been observed in peripheral cells from AD patients and transgenic mice in the absence of Aβ (9, 16, 44, 51). Accordingly, we hypothesize that life-long enhanced $InsP_3R$-mediated Ca^{2+} release is a molecular mechanism, at least in FAD, that drives excessive mitochondrial ROS production with consequent pathological sequelae that result in neuronal impairment and cognitive decline. Testing this hypothesis will require the development of appropriate animals models with features of AD-associated oxidative stress and brain $InsP_3R$ activity modified.

In summary, FAD mutant PS interact with the $InsP_3R$ Ca^{2+} release channel, and through a gain of function, enhance its activity to low levels of $InsP_3$ that may exist constitutively in resting cells, causing exaggerated Ca^{2+} signaling in both the temporal and spatial domains. This Ca^{2+} signaling pathway impinges on mitochondria, enhancing the production of ROS that may, over time, contribute to the pathology of AD.

Acknowledgments

Acknowledgement is made to the donors of Alzheimer's Disease Research, a program of the American Health Assistance Foundation (A2008-137 to J.K.F.), NIH GM56328 and MH059937 to JKF and the Alzheimer's Disease Core Center at the University of Pennsylvania (AG 10124).

Author Disclosure Statement

No competing financial interests exist.

References

1. Annaert W and De Strooper B. Presenilins: Molecular switches between proteolysis and signal transduction. *Trends Neurosci* 22: 439–443, 1999.
2. Atamna H and Frey WH, 2nd. Mechanisms of mitochondrial dysfunction and energy deficiency in Alzheimer's disease. *Mitochondrion* 7: 297–310, 2007.
3. Balaban RS. The role of Ca^{2+} signaling in the coordination of mitochondrial ATP production with cardiac work. *Biochim Biophys Acta* 1787: 1334–1341, 2009.
4. Beal MF. Mitochondria take center stage in aging and neurodegeneration. *Ann Neurol* 58: 495–505, 2005.
5. Brookes PS, Levonen AL, Shiva S, Sarti P, and Darley–Usmar VM. Mitochondria: regulators of signal transduction by reactive oxygen and nitrogen species. *Free Radic Biol Med* 33: 755–764, 2002.
6. Busche MA, Eichhoff G, Adelsberger H, Abramowski D, Wiederhold KH, Haass C, Staufenbiel M, Konnerth A, and Garaschuk O. Clusters of hyperactive neurons near amyloid plaques in a mouse model of Alzheimer's disease. *Science* 321: 1686–1689, 2008.
7. Buxbaum JD, Ruefli AA, Parker CA, Cypess AM, and Greengard P. Calcium regulates processing of the Alzheimer amyloid protein precursor in a protein kinase C-independent manner. *Proc Natl Acad Sci USA* 91: 4489–4493, 1994.
8. Cardenas C, Miller R, Smith I, Bui T, Molgo J, Muller M, Vais H, Cheung KH, Yang J, Parker I, Thompson CB, Birnbaum M, Hallows KR, and Foskett JK. Essential regulation of cell bioenergetics by constitutive $InsP_3$ receptor Ca^{2+} transfer to mitochondria. *Cell* 142: 270–283, 2010.
9. Cecchi C, Latorraca S, Sorbi S, Iantomasi T, Favilli F, Vincenzini MT, and Liguri G. Gluthatione level is altered in lymphoblasts from patients with familial Alzheimer's disease. *Neurosci Lett* 275: 152–154, 1999.
10. Chakroborty S, Goussakov I, Miller MB, and Stutzmann GE. Deviant ryanodine receptor-mediated calcium release resets synaptic homeostasis in presymptomatic 3xTg-AD mice. *J Neurosci* 29: 9458–9470, 2009.
11. Chan SL, Mayne M, Holden CP, Geiger JD, and Mattson MP. Presenilin-1 mutations increase levels of ryanodine receptors and calcium release in PC12 cells and cortical neurons. *J Biol Chem* 275: 18195–18200, 2000.
12. Cheung KH, Mei L, Mak DO, Hayashi I, Iwatsubo T, Kang DE, and Foskett JK. Gain-of-function enhancement of IP_3 receptor modal gating by familial Alzheimer's disease-linked presenilin mutants in human cells and mouse neurons. *Sci Signal* 3: ra22, 2010.
13. Cheung KH, Shineman D, Muller M, Cardenas C, Mei L, Yang J, Tomita T, Iwatsubo T, Lee VM, and Foskett JK. Mechanism of Ca^{2+} disruption in Alzheimer's disease by presenilin regulation of $InsP_3$ receptor channel gating. *Neuron* 58: 871–883, 2008.

14. De Strooper B, Saftig P, Craessaerts K, Vanderstichele H, Guhde G, Annaert W, Von Figura K, and Van Leuven F. Deficiency of presenilin-1 inhibits the normal cleavage of amyloid precursor protein. *Nature* 391: 387–390, 1998.
15. Duchen MR. Mitochondria and calcium: From cell signalling to cell death. *J Physiol* 529: 57–68, 2000.
16. Eckert A, Schindowski K, Leutner S, Luckhaus C, Touchet N, Czech C, and Muller WE. Alzheimer's disease-like alterations in peripheral cells from presenilin-1 transgenic mice. *Neurobiol Dis* 8: 331–342, 2001.
17. Etcheberrigaray R, Hirashima N, Nee L, Prince J, Govoni S, Racchi M, Tanzi RE, and Alkon DL. Calcium responses in fibroblasts from asymptomatic members of Alzheimer's disease families. *Neurobiol Dis* 5: 37–45, 1998.
18. Feissner RF, Skalska J, Gaum WE, and Sheu SS. Crosstalk signaling between mitochondrial Ca^{2+} and ROS. *Front Biosci* 14: 1197–1218, 2009.
19. Forman MS, Trojanowski JQ, and Lee VM. Neurodegenerative diseases: A decade of discoveries paves the way for therapeutic breakthroughs. *Nat Med* 10: 1055–1063, 2004.
20. Foskett JK, White C, Cheung KH, and Mak DO. Inositol trisphosphate receptor Ca^{2+} release channels. *Physiol Rev* 87: 593–658, 2007.
21. Gibson GE and Huang HM. Mitochondrial enzymes and endoplasmic reticulum calcium stores as targets of oxidative stress in neurodegenerative diseases. *J Bioenerg Biomembr* 36: 335–340, 2004.
22. Gibson GE and Huang HM. Oxidative stress in Alzheimer's disease. *Neurobiol Aging* 26: 575–578, 2005.
23. Green KN, Demuro A, Akbari Y, Hitt BD, Smith IF, Parker I, and LaFerla FM. SERCA pump activity is physiologically regulated by presenilin and regulates amyloid beta production. *J Gen Physiol* 132: i1, 2008.
24. Guo Q, Christakos S, Robinson N, and Mattson MP. Calbindin D28k blocks the proapoptotic actions of mutant presenilin 1: Reduced oxidative stress and preserved mitochondrial function. *Proc Natl Acad Sci USA* 95: 3227–3232, 1998.
25. Guo Q, Fu W, Holtsberg FW, Steiner SM, and Mattson MP. Superoxide mediates the cell-death-enhancing action of presenilin-1 mutations. *J Neurosci Res* 56: 457–470, 1999.
26. Guo Q, Sebastian L, Sopher BL, Miller MW, Ware CB, Martin GM, and Mattson MP. Increased vulnerability of hippocampal neurons from presenilin-1 mutant knock-in mice to amyloid beta-peptide toxicity: Central roles of superoxide production and caspase activation. *J Neurochem* 72: 1019–1029, 1999.
27. Haass C and Selkoe DJ. Soluble protein oligomers in neurodegeneration: Lessons from the Alzheimer's amyloid beta-peptide. *Nat Rev Mol Cell Biol* 8: 101–112, 2007.
28. Hajnoczky G, Robb–Gaspers LD, Seitz MB, and Thomas AP. Decoding of cytosolic calcium oscillations in the mitochondria. *Cell* 82: 415–424, 1995.
29. Hardy J and Selkoe DJ. The amyloid hypothesis of Alzheimer's disease: Progress and problems on the road to therapeutics. *Science* 297: 353–356, 2002.
30. Herms J, Schneider I, Dewachter I, Caluwaerts N, Kretzschmar H, and Van Leuven F. Capacitive calcium entry is directly attenuated by mutant presenilin-1, independent of the expression of the amyloid precursor protein. *J Biol Chem* 278: 2484–2489, 2003.
31. Hirashima N, Etcheberrigaray R, Bergamaschi S, Racchi M, Battaini F, Binetti G, Govoni S, and Alkon DL. Calcium responses in human fibroblasts: A diagnostic molecular profile for Alzheimer's disease. *Neurobiol Aging* 17: 549–555, 1996.
32. Hoglinger GU, Breunig JJ, Depboylu C, Rouaux C, Michel PP, Alvarez–Fischer D, Boutillier AL, Degregori J, Oertel WH, Rakic P, Hirsch EC, and Hunot S. The pRb/E2F cell-cycle pathway mediates cell death in Parkinson's disease. *Proc Natl Acad Sci USA* 104: 3585–3590, 2007.
33. Huang HM, Ou HC, and Hsueh SJ. Amyloid beta peptide enhanced bradykinin-mediated inositol (1,4,5) trisphosphate formation and cytosolic free calcium. *Life Sci* 63: 195–203, 1998.
34. Ionescu L, White C, Cheung KH, Shuai J, Parker I, Pearson JE, Foskett JK, and Mak DO. Mode switching is the major mechanism of ligand regulation of $InsP_3$ receptor calcium release channels. *J Gen Physiol* 130: 631–645, 2007.
35. Ito E, Oka K, Etcheberrigaray R, Nelson TJ, McPhie DL, Tofel–Grehl B, Gibson GE, and Alkon DL. Internal Ca^{2+} mobilization is altered in fibroblasts from patients with Alzheimer disease. *Proc Natl Acad Sci USA* 91: 534–538, 1994.
36. Kasri NN, Kocks SL, Verbert L, Hebert SS, Callewaert G, Parys JB, Missiaen L, and De Smedt H. Up-regulation of inositol 1,4,5-trisphosphate receptor type 1 is responsible for a decreased endoplasmic-reticulum Ca^{2+} content in presenilin double knock-out cells. *Cell Calcium* 40: 41–51, 2006.
37. Kemmerling U, Munoz P, Muller M, Sanchez G, Aylwin ML, Klann E, Carrasco MA, and Hidalgo C. Calcium release by ryanodine receptors mediates hydrogen peroxide-induced activation of ERK and CREB phosphorylation in N2a cells and hippocampal neurons. *Cell Calcium* 41: 491–502, 2007.
38. Kuchibhotla KV, Goldman ST, Lattarulo CR, Wu HY, Hyman BT, and Bacskai BJ. Abeta plaques lead to aberrant regulation of calcium homeostasis *in vivo* resulting in structural and functional disruption of neuronal networks. *Neuron* 59: 214–225, 2008.
39. Kuchibhotla KV, Lattarulo CR, Hyman BT, and Bacskai BJ. Synchronous hyperactivity and intercellular calcium waves in astrocytes in Alzheimer mice. *Science* 323: 1211–1215, 2009.
40. LaFerla FM. Calcium dyshomeostasis and intracellular signalling in Alzheimer's disease. *Nat Rev Neurosci* 3: 862–872, 2002.
41. Leissring MA, Akbari Y, Fanger CM, Cahalan MD, Mattson MP, and LaFerla FM. Capacitative calcium entry deficits and elevated luminal calcium content in mutant presenilin-1 knockin mice. *J Cell Biol* 149: 793–798, 2000.
42. Leissring MA, LaFerla FM, Callamaras N, and Parker I. Subcellular mechanisms of presenilin-mediated enhancement of calcium signaling. *Neurobiol Dis* 8: 469–478, 2001.
43. Leissring MA, Paul BA, Parker I, Cotman CW, and LaFerla FM. Alzheimer's presenilin-1 mutation potentiates inositol 1,4,5-trisphosphate-mediated calcium signaling in Xenopus oocytes. *J Neurochem* 72: 1061–1068, 1999.
44. Leutner S, Schindowski K, Frolich L, Maurer K, Kratzsch T, Eckert A, and Muller WE. Enhanced ROS-generation in lymphocytes from Alzheimer's patients. *Pharmacopsychiatry* 38: 312–315, 2005.
45. Li H, Wolfe MS, and Selkoe DJ. Toward structural elucidation of the gamma-secretase complex. *Structure* 17: 326–334, 2009.
46. Mak D–OD, White C, Ionescu L, and Foskett JK. Nuclear patch clamp electrophysiology of inositol trisphosphate receptor Ca^{2+} release channels. In: *Methods in Calcium Signaling Research*. edited by Putney JW J. Boca Raton: CRC Press; 2005.
47. Mark RJ, Hensley K, Butterfield DA, and Mattson MP. Amyloid beta-peptide impairs ion-motive ATPase activities:

Evidence for a role in loss of neuronal Ca^{2+} homeostasis and cell death. *J Neurosci* 15: 6239–6249, 1995.
48. Mattson MP. Pathways towards and away from Alzheimer's disease. *Nature* 430: 631–639, 2004.
49. Mattson MP and Guo Q. Cell and molecular neurobiology of presenilins: A role for the endoplasmic reticulum in the pathogenesis of Alzheimer's disease? *J Neurosci Res* 50: 505–513, 1997.
50. McCormack JG, Halestrap AP, and Denton RM. Role of calcium ions in regulation of mammalian intramitochondrial metabolism. *Physiol Rev* 70: 391–425, 1990.
51. Migliore L, Fontana I, Trippi F, Colognato R, Coppede F, Tognoni G, Nucciarone B, and Siciliano G. Oxidative DNA damage in peripheral leukocytes of mild cognitive impairment and AD patients. *Neurobiol Aging* 26: 567–573, 2005.
52. Miquel J, Economos AC, Fleming J, and Johnson JE, Jr. Mitochondrial role in cell aging. *Exp Gerontol* 15: 575–591, 1980.
53. Mogensen HS, Beatty DM, Morris SJ, and Jorgensen OS. Amyloid beta-peptide (25–35) changes Ca^{2+} in hippocampal neurons. *Neuroreport* 9: 1553–1558, 1998.
54. Nelson O, Tu H, Lei T, Bentahir M, de Strooper B, and Bezprozvanny I. Familial Alzheimer disease-linked mutations specifically disrupt Ca^{2+} leak function of presenilin 1. *J Clin Invest* 117: 1230–1239, 2007.
55. Nunomura A, Castellani RJ, Lee HG, Moreira PI, Zhu X, Perry G, and Smith MA. Neuropathology in Alzheimer's disease: Awaking from a hundred-year-old dream. *Sci Aging Knowledge Environ* 2006: pe10, 2006.
56. Nunomura A, Castellani RJ, Zhu X, Moreira PI, Perry G, and Smith MA. Involvement of oxidative stress in Alzheimer disease. *J Neuropathol Exp Neurol* 65: 631–641, 2006.
57. Querfurth HW and Selkoe DJ. Calcium ionophore increases amyloid beta peptide production by cultured cells. *Biochemistry* 33: 4550–4561, 1994.
58. Reddy PH. Amyloid precursor protein-mediated free radicals and oxidative damage: Implications for the development and progression of Alzheimer's disease. *J Neurochem* 96: 1–13, 2006.
59. Reddy PH and Beal MF. Are mitochondria critical in the pathogenesis of Alzheimer's disease? *Brain Res Brain Res Rev* 49: 618–632, 2005.
60. Rizzuto R, Brini M, Murgia M, and Pozzan T. Microdomains with high Ca^{2+} close to IP3-sensitive channels that are sensed by neighboring mitochondria. *Science* 262: 744–747, 1993.
61. Rizzuto R, Pinton P, Carrington W, Fay FS, Fogarty KE, Lifshitz LM, Tuft RA, and Pozzan T. Close contacts with the endoplasmic reticulum as determinants of mitochondrial Ca^{2+} responses. *Science* 280: 1763–1766, 1998.
62. Schapira AH. Mitochondrial dysfunction in neurodegenerative disorders. *Biochim Biophys Acta* 1366: 225–233, 1998.
63. Serrano F and Klann E. Reactive oxygen species and synaptic plasticity in the aging hippocampus. *Ageing Res Rev* 3: 431–443, 2004.
64. Smith IF, Green KN, and LaFerla FM. Calcium dysregulation in Alzheimer's disease: Recent advances gained from genetically modified animals. *Cell Calcium* 38: 427–437, 2005.
65. Smith IF, Hitt B, Green KN, Oddo S, and LaFerla FM. Enhanced caffeine-induced Ca^{2+} release in the 3xTg-AD mouse model of Alzheimer's disease. *J Neurochem* 94: 1711–1718, 2005.
66. Smith MA, Rottkamp CA, Nunomura A, Raina AK, and Perry G. Oxidative stress in Alzheimer's disease. *Biochim Biophys Acta* 1502: 139–144, 2000.
67. Spat A, Szanda G, Csordas G, and Hajnoczky G. High- and low-calcium-dependent mechanisms of mitochondrial calcium signalling. *Cell Calcium* 44: 51–63, 2008.
68. Stutzmann GE. Calcium dysregulation, IP_3 signaling, and Alzheimer's disease. *Neuroscientist* 11: 110–115, 2005.
69. Stutzmann GE. The pathogenesis of Alzheimers disease. Is it a lifelong "calciumopathy"? *Neuroscientist* 13: 546–559, 2007.
70. Stutzmann GE, Caccamo A, LaFerla FM, and Parker I. Dysregulated IP_3 signaling in cortical neurons of knock-in mice expressing an Alzheimer's-linked mutation in presenilin1 results in exaggerated Ca^{2+} signals and altered membrane excitability. *J Neurosci* 24: 508–513, 2004.
71. Stutzmann GE, Smith I, Caccamo A, Oddo S, Laferla FM, and Parker I. Enhanced ryanodine receptor recruitment contributes to Ca^{2+} disruptions in young, adult, and aged Alzheimer's disease mice. *J Neurosci* 26: 5180–5189, 2006.
72. Stutzmann GE, Smith I, Caccamo A, Oddo S, Parker I, and Laferla F. Enhanced ryanodine-mediated calcium release in mutant PS1-expressing Alzheimer's mouse models. *Ann NY Acad Sci* 1097: 265–277, 2007.
73. Tanzi RE and Bertram L. Twenty years of the Alzheimer's disease amyloid hypothesis: A genetic perspective. *Cell* 120: 545–555, 2005.
74. Terada LS. Specificity in reactive oxidant signaling: Think globally, act locally. *J Cell Biol* 174: 615–623, 2006.
75. Tu H, Nelson O, Bezprozvanny A, Wang Z, Lee SF, Hao YH, Serneels L, De Strooper B, Yu G, and Bezprozvanny I. Presenilins form ER Ca^{2+} leak channels, a function disrupted by familial Alzheimer's disease-linked mutations. *Cell* 126: 981–993, 2006.
76. White C, Li C, Yang J, Petrenko NB, Madesh M, Thompson CB, and Foskett JK. The endoplasmic reticulum gateway to apoptosis by Bcl-x_L modulation of the $InsP_3R$. *Nat Cell Biol* 7: 1021–1028, 2005.
77. Xia W, Zhang J, Perez R, Koo EH, and Selkoe DJ. Interaction between amyloid precursor protein and presenilins in mammalian cells: Implications for the pathogenesis of Alzheimer disease. *Proc Natl Acad Sci USA* 94: 8208–8213, 1997.
78. Yoo AS, Cheng I, Chung S, Grenfell TZ, Lee H, Pack–Chung E, Handler M, Shen J, Xia W, Tesco G, Saunders AJ, Ding K, Frosch MP, Tanzi RE, and Kim TW. Presenilin-mediated modulation of capacitative calcium entry. *Neuron* 27: 561–572, 2000.

Address correspondence to:
J. Kevin Foskett, Ph.D.
Department of Physiology
B39 Anatomy-Chemistry Building
University of Pennsylvania
Philadelphia, PA 19104-6085

E-mail: foskett@mail.med.upenn.edu

Date of first submission to ARS Central, July 1, 2010; date of final revised submission, August 2, 2010; date of acceptance, August 10, 2010.

Abbreviations Used

Aβ = beta-amyloid
AD = Alzheimer's disease
APP = amyloid precursor protein
ATP = adenosine 5′-triphosphate
BAPTA = 1,2-bis(o-aminophenoxy) ethane-N,N,N′,N′-tetraacetic acid
BCR = B cell receptor
Ca^{2+} = calcium
CICR = calcium-induced calcium release
ER = endoplasmic reticulum
FAD = familial Alzheimer's disease
H_2O_2 = hydrogen peroxide
$InsP_3$ = inositol 1,4,5-trisphosphate
$InsP_3R$ = inositol 1,4,5-trisphosphate receptor
KO = knock-out
LTP = long-term potentiation
PS1 = presenilin 1
PS2 = presenilin 2
ROS = reactive oxygen species
RyR = ryanodine receptor
SERCA = sarco/endoplasmic calcium ATPase
TCA = tricarboxylic acid
WT = wild type

This article has been cited by:

1. Nicola Sassi, Lucia Biasutto, Andrea Mattarei, Massimo Carraro, Valentina Giorgio, Anna Citta, Paolo Bernardi, Spiridione Garbisa, Ildikò Szabò, Cristina Paradisi, Mario Zoratti. 2012. Cytotoxicity of a mitochondriotropic quercetin derivative: Mechanisms. *Biochimica et Biophysica Acta (BBA) - Bioenergetics* **1817**:7, 1095-1106. [CrossRef]
2. Santeri Kiviluoto, Haidar Akl, Tim Vervliet, Geert Bultynck, Jan B. Parys, Ludwig Missiaen, Humbert De Smedt. 2012. IP3 receptor-binding partners in cell-death mechanisms. *Wiley Interdisciplinary Reviews: Membrane Transport and Signaling* **1**:2, 201-210. [CrossRef]
3. Denise Riquelme , Alvaro Alvarez , Nancy Leal , Tatiana Adasme , Italo Espinoza , Juan Antonio Valdés , Natalia Troncoso , Steffen Hartel , Jorge Hidalgo , Cecilia Hidalgo , M. Angélica Carrasco . 2011. High-Frequency Field Stimulation of Primary Neurons Enhances Ryanodine Receptor-Mediated Ca2+ Release and Generates Hydrogen Peroxide, Which Jointly Stimulate NF-#B Activity. *Antioxidants & Redox Signaling* **14**:7, 1245-1259. [Abstract] [Full Text HTML] [Full Text PDF] [Full Text PDF with Links] [Supplemental material]
4. Andrea C. Paula-Lima , Tatiana Adasme , Carol SanMartín , Adriano Sebollela , Claudio Hetz , M. Angélica Carrasco , Sergio T. Ferreira , Cecilia Hidalgo . 2011. Amyloid #-Peptide Oligomers Stimulate RyR-Mediated Ca2+ Release Inducing Mitochondrial Fragmentation in Hippocampal Neurons and Prevent RyR-Mediated Dendritic Spine Remodeling Produced by BDNF. *Antioxidants & Redox Signaling* **14**:7, 1209-1223. [Abstract] [Full Text HTML] [Full Text PDF] [Full Text PDF with Links] [Supplemental material]
5. Cecilia Hidalgo , M. Angélica Carrasco . 2011. Redox Control of Brain Calcium in Health and Disease. *Antioxidants & Redox Signaling* **14**:7, 1203-1207. [Abstract] [Full Text HTML] [Full Text PDF] [Full Text PDF with Links]
6. Jean-Paul Decuypere, Giovanni Monaco, Ludwig Missiaen, Humbert De Smedt, Jan B. Parys, Geert Bultynck. 2011. IP3 Receptors, Mitochondria, and Ca2+ Signaling: Implications for Aging. *Journal of Aging Research* **2011**, 1-20. [CrossRef]